G. Hasinger

X-ray Diagnostics of Accretion Disks

1 Introduction

Within this article the very wide field of accretion phenomena observed in X-rays is restricted to bright low-mass X-ray binaries (LMXB), where recent observational evidence leads to a global picture that for the first time sheds light on the innermost regions of an accretion disk. LMXB are actually very similar to cataclysmic variables, one just has to replace the central white dwarf by a neutron star. Given a small enough neutron star magnetosphere the disk then reaches to much smaller radii and therefore much higher temperatures. Consequently, radiation pressure can become important in the inner part of accretion disks around neutron stars.

Table 1 from the recent review by van der Klis (1989b) shows the known LMXB sorted according to apparent X-ray brightness and marked as "Z-sources" and "Atoll-Sources" according to the classification scheme by Hasinger and van der Klis (1989). The class of LMXB we are concerned here – the Z-sources – belong to the brightest X-ray objects in the sky. They are characterized by Z-shaped X-ray colour-colour diagrams and comparatively narrow peaks of quasi-periodic oscillations (QPO) at frequencies between 5 and 50 Hz in their power spectra.

In the recent years it turned out that in the handful Z-sources nature has provided us with a magnificent laboratory to study the innermost regions of accretion disks – not at least at X-ray wavelengths.

Table 1. The brightest low-mass X-ray binaries (adapted from van der Klis, 1989b)

Source Name	I_x [μJy]	P_{orb} [hr]	Type A/Z	Phenomenology
Sco X-1 (1617-155)	12400	19.2	Z	QPO
GX 5-1 (1758-259)	1200	—	Z	QPO
GX 349+2 (1702-363)	780	—	Z	QPO
GX 17+2 (1813-140)	680	19.8?	Z	QPO, (bu)
GX 9+1 (1758-205)	650	—	A	—
GX 340+0 (1642-455)	490	—	Z	QPO
GX 3+1 (1744-265)	430	—	A	(QPO),(Bu)
Cyg X-2 (2142+380)	430	235.	Z	QPO,(bu)
GX 13+1 (1811-171)	340	—	A	—
GX 9+9 (1728-169)	290	4.2	A	Mo
4U 1820-30 (NGC 6624)	260	0.2	A	(QPO),(Bu),Mo
4U 1705-44	260	—	A	Bu
4U 1636-53	220	3.8	A	Bu
Ser X-1 (1837+049)	200	—	-	Bu
GCX-1 (1742-294)	170	—	A	Bu?
4U 1728-33	170	—	A	Bu
GX 339-4 (1659-487)	160	14.8?	-	QPO,BH?
4U 1735-44	160	4.6	A	Bu

2 X-ray Spectrophotometry

The technique we utilize here is rather simple and similar to the UBV spectroscopy in optical astronomy. The raw X-ray spectrum is divided into three rather broad energy bands - typically 1-3 keV, 3-6 keV and 6-15 keV. From the ratio between the middle and the soft X-ray band a so-called *soft colour* is derived, the ratio between the hard and the middle X-ray band gives the *hard colour*.

Figure 1 shows X-ray data from Cyg X-2 measured over four days with the Japanese satellite *Ginga* during a multifrequency campaign in 1988 (from Hasinger et al., 1990, hereafter HA90). The lowest panel shows the X-ray intensity as a function of time, the middle one gives the hard colour. The uppermost panel shows the times of simultaneous observations in other wavebands (see below). Both X-ray intensity and X-ray colour vary quite erratically on a variety of

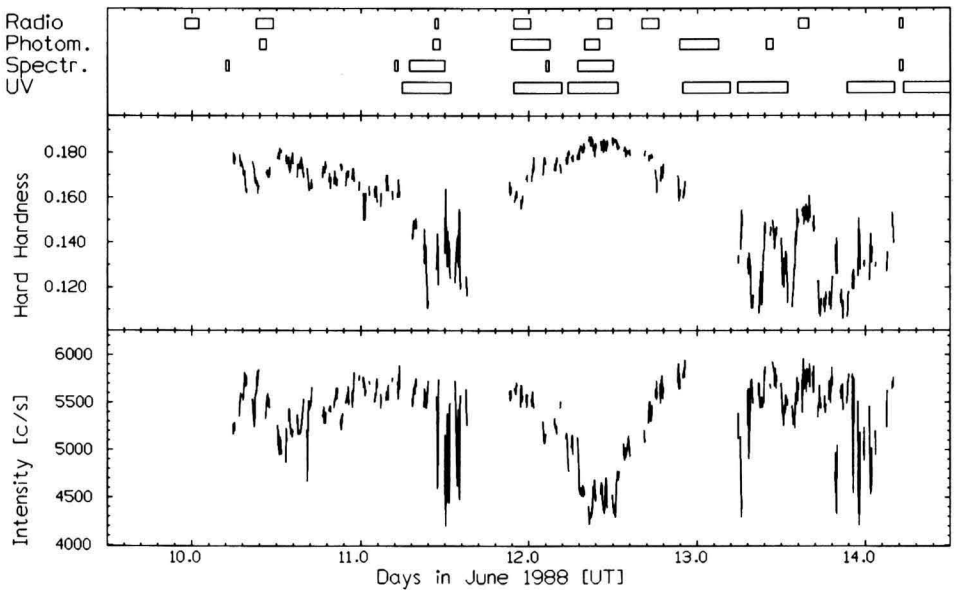

Fig. 1. X-ray lightcurve (lower panel) and hard colour (middle panel) of Cyg X-2 as a function of time for the 4-day Ginga observation in June 1988. The upper panel shows the time interval of observations in other wavebands. Taken from Hasinger et al., 1990

different timescales. However, the source has been observed in different modes of activity. Phases of slowly variing intensity and hardness are interrupted by periods of rapidly variing colour or intensity.

3 The "Z-Diagram"

The chaotic nature of the temporal variability changes into very well structured and characteristic patterns when one plots the same data into a colour-intensity diagram (similar to the Hertzsprung-Russel diagram of optical astronomy) or into a colour-colour diagram. These two diagrams are given in Figs. 1 and 2. Now three well separated "spectral branches" are visible which form an elongated "Z-shape" in the colour-colour diagram which gave these sources their name.

The three branches are called "horizontal branch" (HB; upper left) where the hard colour stays almost constant while the intensity varies, "normal branch" (NB; middle) where both soft and hard colour change in a correlated fashion while the X-ray intensity stays almost constant, and "flaring branch" (FB; bottom) which again is characterized by a correlated variation of soft and hard colour, however along a different track. (The dramatic intensity decrease along the flaring branch is peculiar to Cyg X-2, in most other Z-sources a similarly dramatic intensity increase has been observed, thus the term "flaring".)

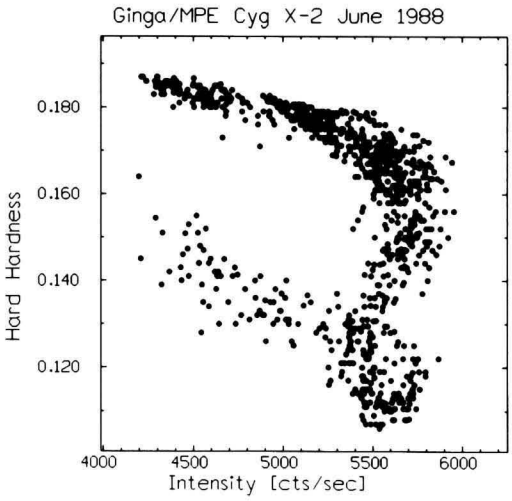

Fig. 2. Colour-intensity diagram from the data in Fig. 1 (HA90)

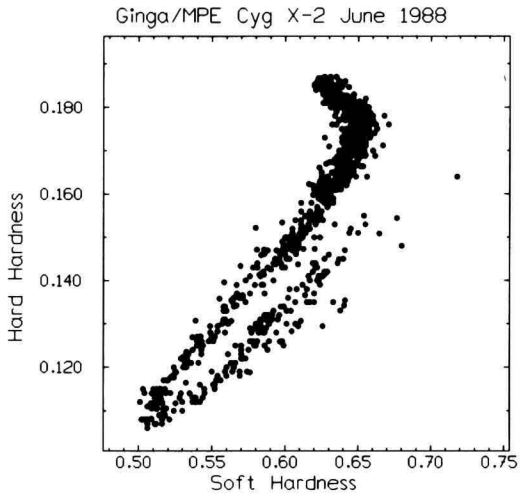

Fig. 3. Colour-colour diagram for the same data (HA90).

The same technique has been applied to a large body of data from the European X-ray satellite EXOSAT (Hasinger and van der Klis, 1989, hereafter HK89) and a total of 6 bright LMXB have been identified as Z-sources. Figure 4 shows their colour-colour diagrams which display a similar complete Z-pattern or at least fragments of it.

The existence of these characteristic, well confined tracks of spectral and intensity evolution calls for a simple explanation. One interpretation assumes that the observed changes are governed by the variation of a single parameter, which most likely is the mass-accretion rate $\dot{M}$ fed through the disk onto the central engine (Priedhorsky et al., 1986). If this is the case, then there are only two choices how $\dot{M}$ can vary along the "Z": either in the "positive" sense (from the upper left to the lower right) or in the opposite direction. In order to solve this question simultaneous observations in other wavebands had to be performed.

4 Observations in Other Wavebands

Simultaneously with the X-ray measurements two multifrequency campaigns with observations of Cyg X-2 in the UV, optical, and radio range have been performed (see figure 1). The IUE observations (Vrtilek et al., 1990), the optical spectroscopy from La Palma (van Paradijs et al., 1990) and the VLA radio measurements (Hjellming et al., 1990) will be published together with the Ginga X-ray data (HA90) soon. Luckily enough the source collaborated: it displayed all three spectral states during the simultaneous observations and

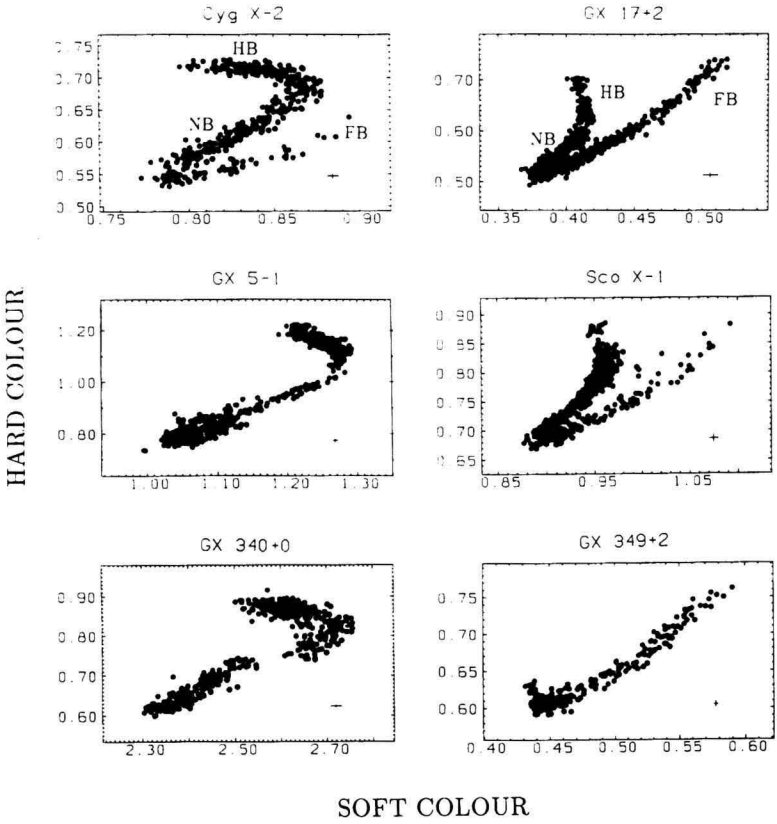

Fig. 4. Colour-colour diagram of EXOSAT data from 6 Z-sources (HK89)

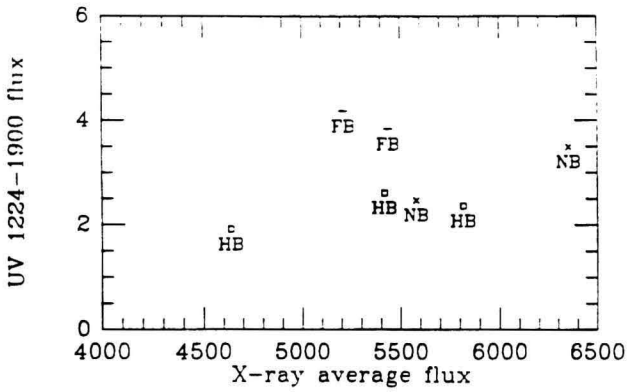

Fig. 5. UV continuum flux as (IUE) versus X-ray flux (Ginga). The X-ray spectral state is indicated for each measurement. The UV flux increases continuously from horizontal to normal branch. Taken from Vrtilek et al., 1990

in all wavebands clear correlations with the source position in the Z-diagram were found.

The UV continuum and line flux increase steadily by a factor of about 2 as the source moves from the horizontal branch to the flaring branch (Vrtilek et al., 1990, see fig. 5). The same is true for the equivalent width of the He II $\lambda 4686$ and $\lambda 4640$ Bowen emission lines as well as the Hβ and Hγ absorption lines (van Paradijs et al., 1990). A similar behaviour was found already in the seventies for Sco X-1, where the optical flux increases by about one magnitude from the top to the bottom of the normal branch normal and further up the flaring branch (Canizares et al., 1975). Since the optical and UV flux of the X-ray irradiated disk is dominated by reprocessed radiation, one can conclude that the X-ray (or EUV) illumination of the disk increases from HB to FB – and thus the mass accretion rate has to increase in the same way (Vrtilek et al., 1990, HA90)

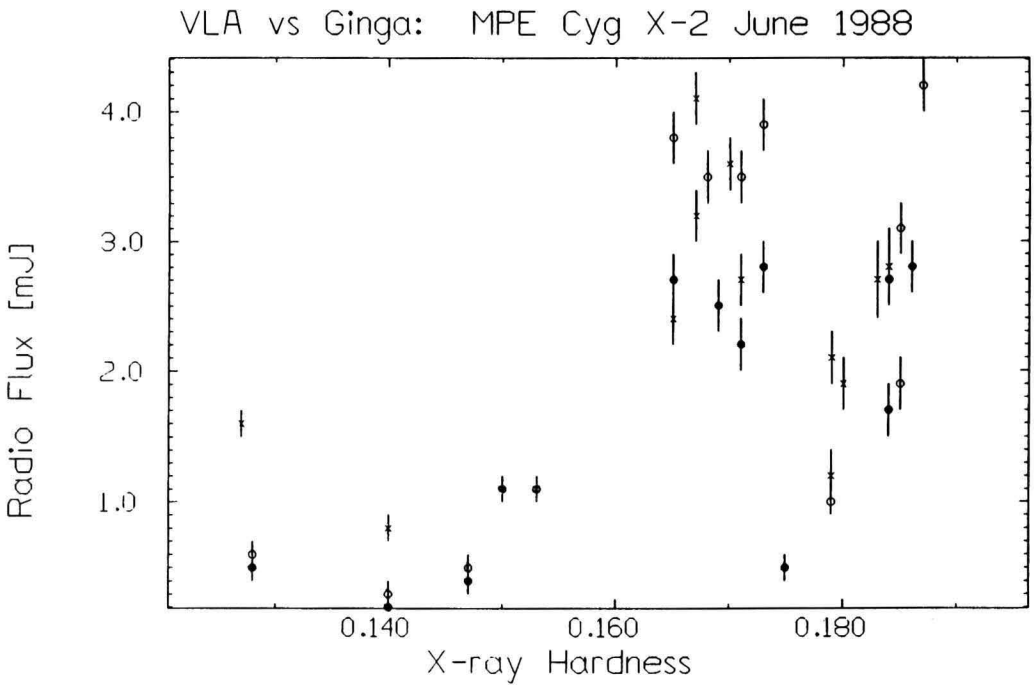

Fig. 6. Radio flux density (VLA) versus X-ray hardness (Ginga). Hardness is the same 'hard hardness' as in fig. 1-3, thus the source is on the horizontal branch for a hardness larger than 0.16. The radio flux density is high and strongly variable on the horizontal branch and low and quiescent on the normal and flaring branch.

The radio flux behaves in a completely different manner: as Figure 6 shows, the radio flux is loud and highly variable on the horizontal branch, and quiet and quiescent on the normal and flaring branch (Hjellming et al., 1990). This is similar as observed before in the radio/X-ray correlation in GX 17+2 (Penninx et al., 1988).

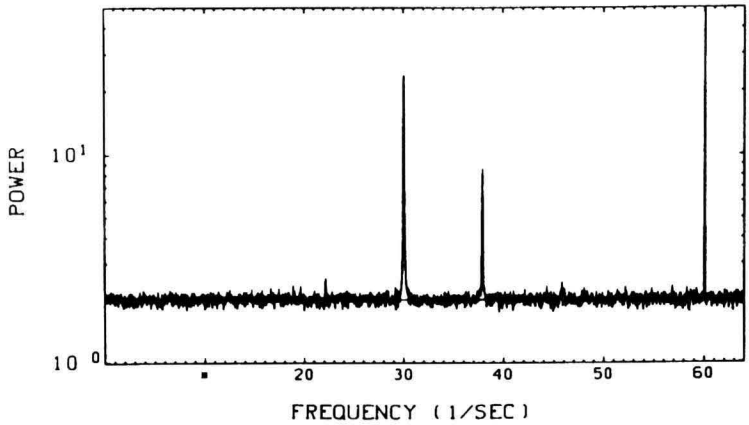

Fig. 6. Power spectrum of the Crab Nebula and its pulsar as observed with EXOSAT. The fundamental pulsar frequency (30 Hz) and its first harmonic (60 Hz) are visible as sharp spikes. A third peak is seen at a frequency of 38Hz, it is the aliased signal of the second harmonic (90 Hz).

5 Quasi-Periodic Oscillations and Noise

The last pieces to solve the puzzle of the Z-sources comes from a systematic analysis of their X-ray flickering in the sub-second range. As diagnostic tool the segmented Fourier analysis technique (see van der Klis, 1989a) is utilized: the observation is divided into small continuous stretches of data (typically 8-32 seconds), the power spectra of which are averaged to enhance the statistical significance of the signal. If this method is applied to the 33ms- pulsar in the Crab Nebula a series of sharp spikes at the fundamental pulsar frequency and its harmonics is observed (see figure 6) on top of a constant (white noise) signal which is due to the counting statistics of the data.

In a search for possible millisecond pulsars in low-mass X-ray binaries van der Klis et al. (1985) analysed data of the bright galactic bulge source GX 5-1. However, instead of several sharp spikes they found a single broad peak in the power spectra, signalling that not a strictly periodic, but a *quasi periodic oscillation* (QPO) is present in the data. Additionally a component called 'red noise' or 'low-frequency noise' (LFN), i.e. excess power which rises continuously towards the lowest frequencies, is visible in the power spectra (see figure 7).

Moreover, as the X-ray source intensity varies, the centroid frequency of the QPO peak is not stable but varies as a function of time, roughly in the frequency range 20-45 Hz – the two quantities go hand in hand.

It turns out, that the presence of QPO peaks in the power spectra is a class property of all Z-sources (see HK89). However, the rapid, intensity-dependent QPO are mainly visible in the horizontal branch. As soon as the source 'turns the corner' into the normal branch the power spectra change dramatically. Figure 8 shows a comparison of two power spectra of Cyg X-2, taken in the horizontal and normal branch, respectively. Compared to figures 6 and 7 the

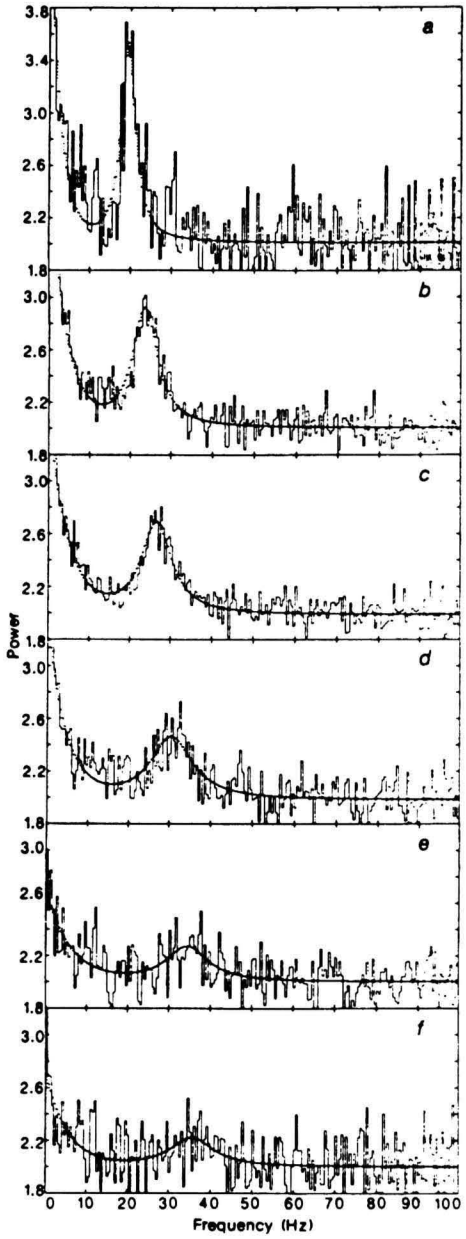

Fig. 7. Six different power spectra of the bright galactic bulge source GX 5-1 in the same representation as figure 6. The X- ray source intensity rises from approximately 2200 cts/s to 3800 cts/sec in the EXOSAT detector from top to bottom (from van der Klis et al., 1985).

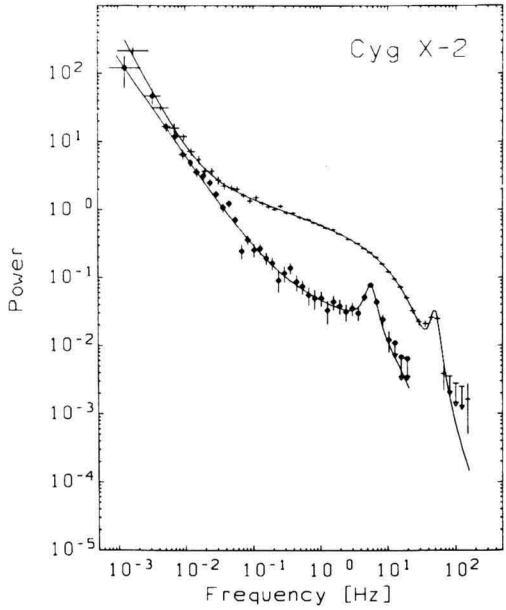

Fig. 8. Two power spectra of the Z-source Cyg X-2 taken in the horizontal (upper) and normal (lower) branch. The power spectra are displayed on a logarithmic scale, with the white noise level due to counting statistics removed. Note that the power spectra are not shifted with respect to each other (from Hasinger, 1987a).

power spectra here are displayed on a logarithmic scale and the white noise due to counting statistics has been subtracted. One sees, that the strong and characteristically shaped low-frequency noise component, dominating in the horizontal branch at frequencies 0.05 - 50 Hz, is almost completely gone in the normal branch. The same is true for the fast (50 Hz) QPO peak. Roughly in the middle of the normal branch another, slower QPO peak occurs, its centroid remains rather stable at frequencies 5-7 Hz throughout the lower part of the normal branch.

These dramatic changes of the different power spectral components are further highlighted in figure 9 where all Cyg X-2 power spectra from the EXOSAT and Ginga X-ray observations have been systematically analysed to trace the source behaviour throughout the whole Z-diagram. Particularly interesting seems the variation of the LFN, which first increases on the horizontal branch and the abruptly dies out close to the HB/NB-corner. This transition has become one of the most important ingredients in the interpretation discussed below. The changes in the HBO (horizontal-branch oscillation) and NBO (normal-branch oscillation) power are anticorrelated, while the former continuously decreases from HB to NB, the latter increases abruptly along the normal branch and is most prominent in the middle of the NB. There are actually NB power spectra which show both HBO and NBO peaks simultaneously (HA90).

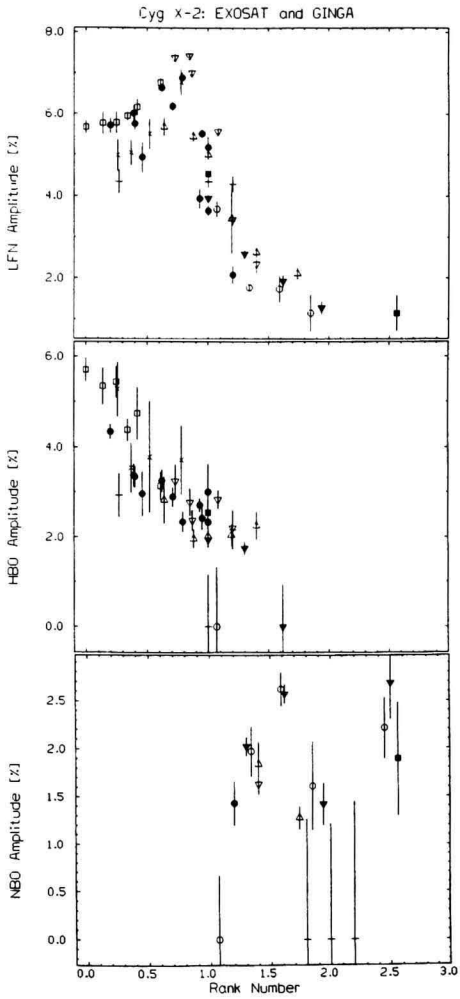

Fig. 9. Variation of the main power spectral components of Cyg X-2. The figures display the rms. variability in the red noise (upper), in the horizontal-branch QPO (middle) and in the normal- branch QPO (lower panel) as a function of position along the Z- diagram. The abscissa (called 'rank number') gives an arbitrary coordinate that increases monotonically from the left of the HB (0.0) over the HB/NB-transition (1.0) and the NB/FB-transition (2.0) to the upper right of the flaring branch (3.0), following the change in mass-accretion rate. Data from the EXOSAT and Ginga X-ray satellites have been merged (Hasinger, et al. 1990, in prep.

The same analysis applied to other Z-sources reveals almost carbon-copy results. Figure 10 shows a selection of power spectra from the same set of sources the colour-colour diagrams of which are given in figure 4 (HK89). Where available, power spectra have been accumulated separately for each branch. The sense and magnitude of variation in the different power spectral components is very similar to Cyg X-2.

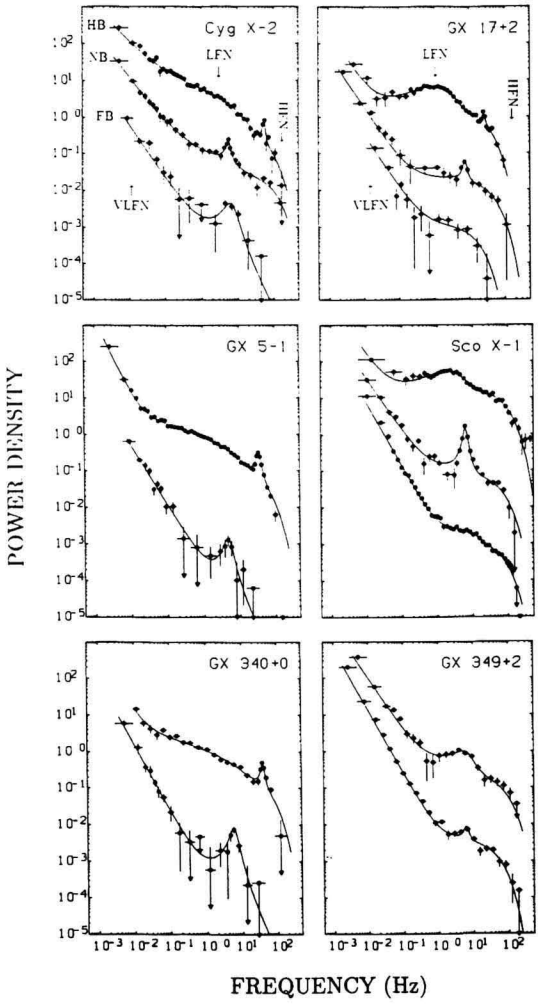

Fig. 10. Power spectra of six Z-sources in the different spectral branches, corresponding to figure 4. Power spectra are given on logarithmic scales with white noise background subtracted. For clarity power spectra from different branches (from top to bottom: HB, NB, FB) are shifted by two decades with respect to each other (from HK89).

6 The Big Picture: a Jumping Accretion Disk ?

Figure 11 summarises the complex variation of some of the observable quantities as a function of mass accretion rate along the Z-diagram: $\dot{M}$ increases monotonically from HB to FB by about a factor of 2 (panel 1). The UV and blue optical light and the emission lines follow hand in hand (panel 2). This is also true for the X-ray flux on the horizontal branch, however, at the HB/NB

transition it starts to deviate from this one-to-one correspondence (panel 3). The latter three quantities all show marked transitions close to the corner between horizontal and flaring branch: horizontal-branch QPO and normal branch QPO change importance in the upper normal branch, where they can coexist simultaneously (panel 4). The LFN, which is strong on the HB, dies out at the same transition (panel 5; see also Figure 9), and finally, strong nonthermal radio flares occur only on the horizontal branch.

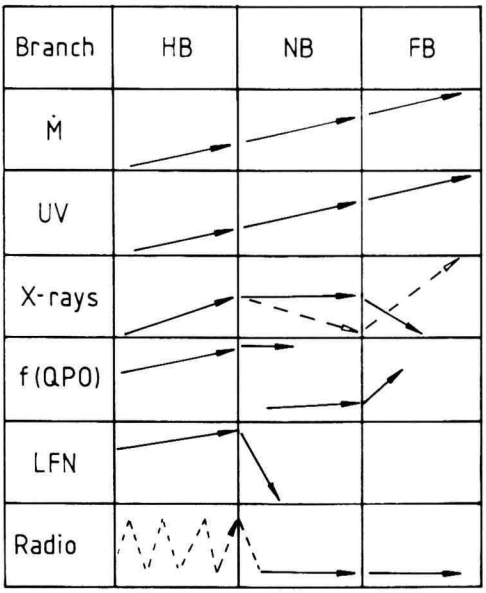

Fig. 11. Schematic display of the variation of important observables and the mass-accretion rate as a function of source position along the Z-profile (see text) (from HA90).

We have now collected the ingredients neccessary to to interpret the complex spectral, power spectral and multifrequency behaviour of Z-sources. Most important is the knowledge that the observed variations are most likely driven by a simple change of mass accretion rate. The second most important feature - at least in my judgement - is the dramatic phase transition when the source moves from the horizontal to the normal branch. X-ray spectrum, and intensity, noise and QPO as well as the radio flux all change dramatically and almost simultaneously there. These phenomena suggest a scenario (Hasinger 1988, HA90), which is sketched in Figure 12, and which is similar to the 'unified QPO model' by Lamb (1989, 1990) in some important features.

At low accretion rates (HB) the source starts out in a configuration with a geometrically thin inner disk which is cutting into a small magnetosphere as shown in figure 12a. This is the geometry required for the 'accretion modulated beat frequency model' for the horizontal-branch QPO (Alpar and Shaham, 1985; Lamb et al., 1985). Turbulence at the magnetospheric boundary

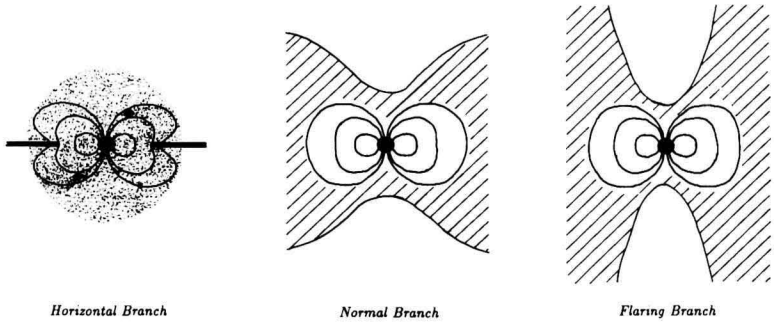

Fig. 12. Schematic display of the accretion geometry in the adopted scenario for the (a) horizontal, (b) normal, and (c) flaring branch (from HA90).

produces clumps, causing an instationary accretion which is responsible for the LFN. Interaction between the clumps in Keplerian motion and between the rotating neutron star magnetic field cause quasi-periodic intensity enhancements leading to HBO. The turbulent magnetospheric boundary may also be the site of electron acceleration which we observe through the HB radio flares.

When a critical value of mass accretion rate is exceeded, but still well below the neutron star Eddington limit, the inner disk is suddenly flaring up to form a thick torus (see Fig. 12b), engulfing the whole magnetosphere (Hasinger, 1988; HK 1989). All the dramatic changes observed at this transition can be explained by this postulated instability. The additional cool disk material in the line of sight causes the softening of the observed spectrum by Compton degradation (Hasinger, 1987b; Lamb, 1990). The interface between the disk torus and the magnetosphere is probably much less turbulent than in the horizontal branch and matter can accrete smoothly onto the neutron star. Therefore LFN and HB QPO are reduced in strength (although the existence of weak HB QPO in the upper normal branch indicates that some inhomogeneities are still present). The flux of energetic electrons producing the HB radio flares may be quenched in two ways: first, the reduced turbulence at the magnetospheric boundary may be less efficient in accelerating particles, and second, the thick inner disk torus will trap the electrons.

Down the normal branch the mass accretion rate is increasing even further and approaches the Eddington limit. At this moment the effective gravity is reduced by the strong radiation pressure, enough to slow down the dynamic timescales so that sound waves (Hasinger 1987a, Alpar et al., 1990) or other resonances in the flow (Lamb 1989, 1990) will become important and possibly form the 6 Hz normal-branch QPO.

Finally, on the flaring branch the mass accretion rate has increased above the Eddington limit and matter will be ejected, probably through the narrow funnel formed by the thick inner disk torus (see Fig. 12c). The funnel might

also effectively beam the X-ray radiation, so that the line-of sight inclination becomes important for a distant observer. This may explain the different intensity behaviour on the flaring branch between e.g. Sco X-1 and Cyg X-2 (Hasinger et al., 1989)

References

Alpar, M.A., Shaham, J.: 1985, *Nature* **316**, 239
Alpar, M.A., Hasinger, G., Shaham, J., Yancopoulos, S., 1990 (in prep.)
Canizares C.R. et al.: 1975 *Ap. J.* **197**, 457
Hasinger, G.: 1987 a, *Astron. Astrophys.* **186**, 153.
Hasinger, G.: 1987 b, *IAU Symp.* **125**, 333.
Hasinger, G.: 1988 Proc. Symp. *"Physics of Neutron Stars and Black Holes"*, Tokyo: Universal Academy Press, p. 97
Hasinger, G., Priedhorsky, W.C., Middleditch, J.: 1989, *Ap. J.* **337**, 843.
Hasinger, G., van der Klis, M.: 1989, *Astron. Astrophys.* **225**, 79
Hasinger, G., van der Klis, M., Ebisawa, K., Dotani, T., Mitsuda, K.: 1990 *Astron. Astrophys.* (in press)
Hjellming, R.M., Han, X.H., Cordova, F.A., Hasinger, G.: 1990 *Astron. Astrophys.* (in press)
Lamb, F.K., Shibazaki, N., Alpar, M.A., Shaham, J.: 1985 *Nature* **317**, 681
Lamb, F.K.: 1989, Proc. 23rd ESLAB Symposium, ESA SP-296, Part 1., p. 215
Lamb, F.K.: 1990, *Ap. J.* (in press)
Penninx, W., Lewin, W.H.G., Zijlstra, A.A., Mitsuda, K., van Paradijs, J., van der Klis, M.: 1988 *Nature* **336**, 146
Priedhorsky, W., Hasinger, G., Lewin, W.H.G., Middleditch, J., Parmar, A., Stella, L., White, N.: 1986, *Ap. J. Lett.* **306**, L91.
Shakura, N.I., Sunyaev, R.A.: 1973 *Astron. Astrophys.* **24**, 337
Van der Klis, M., Jansen, F., van Paradijs, J., Lewin, W.H.G., van den Heuvel, E.P.J., Trümper, J.E., and Sztajno, M.: 1985 *Nature* **316**, 225.
Van der Klis, M.: 1989a, Proc. NATO ASI *"Timing Neutron Stars"*, Çeşme, Turkey. Dordrecht: Reidel p.27
Van der Klis, M.: 1989b, *Ann. Rev. Astron. Astrophys.* **27**, 517
Van Paradijs, J., Allington-Smith, J., Callanan, P., Charles, P.A., Hassal, B.J.M., Machin, G., Mason, K.O., Naylor, T., Smale, A.P.: 1990 *Astron. Astrophys.* (in press)
Vrtilek, S.D., Raymond, J.C., Garcia, M.R., Verbunt, F., Hasinger, G., Kürster, M.: 1990 *Astron. Astrophys.* (in press)

This article was processed by the author using the TEX Macropackage from Springer-Verlag.

Max-Planck-Institut für extraterrestrische Physik, 8046 Garching, FRG